INVITED PAPER Special Section on Josephson Junctions — Past 50 years and Future —

Terahertz Radiation Emitted from Intrinsic Josephson Junctions in High-T_c Superconductor $Bi_2Sr_2CaCu_2O_{8+\delta}$

Hidetoshi MINAMI[†a)], **Manabu TSUJIMOTO**[†], **Takanari KASHIWAGI**[†], **Takashi YAMAMOTO**[†*], *and* **Kazuo KADOWAKI**[†], *Nonmembers*

SUMMARY The present status of superconducting terahertz emitter using the intrinsic Josephson junctions in high-T_c superconductor $Bi_2Sr_2CaCu_2O_{8+\delta}$ is reviewed. Fabrication methods of the emitting device, electrical and optical characteristics of them, synchronizing operation of two emitters and an example of applications to the terahertz imaging will be discussed. After the description of fabrication techniques by an Argon ion milling with photolithography or metal masks and by a focused ion beam, optical properties of radiation spectra, the line width, polarization and the spatial distribution of emission are presented with some discussion on the operation mechanism. For electrical properties, reversible and irreversible operations at high and low electrical currents, respectively, and electrical modulation of the radiation intensity for terahertz imaging are presented.

key words: *intrinsic Josephson junction, terahertz, high-T_c, superconductor*

1. Introduction

The frequency range approximately from 100 GHz up to several THz has attracted much attention because of a variety of useful potential applications such as spectroscopic analyses, various kinds of nondestructive sensing and imaging, medical diagnoses, security controls and high speed communication, etc. [1], [2]. Although they are highly demanded, a lack of compact, convenient and inexpensive solid-state emitters as well as the sensitive detectors at this frequency range hinders development, known as the THz gap.

A Josephson junction as a quantum device enables us to make ultrahigh frequency devices due to their extremely fast response, for examples, high precision voltage standards, multiplexers, mixers and excellently high sensitive electromagnetic-wave detectors, etc. at the frequency range from 10 GHz up to several THz. It is a well-known fact that in a Josephson junction the *ac*-Josephson effect works as a natural voltage-frequency transducer which transforms a *dc*-voltage to a high-frequency *ac*-current, described by the formula $f=(2e/h)V=483.597891$ GHz/mV, where f is the frequency of the *ac*-Josephson current, V the *dc*-voltage appearing two superconducting electrodes, e the elementary charge, and h Planck constant. Thus, the Josephson junction can be an excellent source of continuous and monochromatic high-frequency electromagnetic radiation. However, the output power detected from a single Josephson junction is ranging from 10^{-12} W to 10^{-10} W so that it was too low for fundamental as well as applied researches [3]–[5].

Considerable power of electromagnetic waves has been demonstrated by the integrated Josephson junction arrays [6]–[17]. The power of about 400 μW at 410 GHz generated from an array of 498 $Nb/AlO_x/Nb$ discrete Josephson junctions was detected by the on-chip detector [12]. This indicates a possible generation of the milliwatt power at submm wavelengths. However, it was only 2 μW at 76 GHz in the off-chip detection for a low-T_c junction array [17], showing the difficulty of coupling to free space for radiation. It is obvious that high power can be obtained when the mutual phase locking of the Josephson currents produced in each junction is achieved in the whole array. Indeed, the coherent emission due to the synchronized Josephson junctions has been confirmed in many cases since the emission power is proportional to the quadratic number of junctions, N^2 [6], [7], [14], [17]. The arrays are also expected to reduce the linewidth by $1/N$. Arrays of discrete Josephson junctions of high-T_c superconductors have been also studied intensively because of possible emissions at higher frequencies up to several THz. The phase-locked operation has been demonstrated [13], however, there have been hurdles to fabricate the larger-scale arrays necessary for more than μW level of radiation, because of the extremely short coherence lengths (the order of Å~ 10 Å) and the difficulty to fabricate identical junctions from multi-element compounds.

A solution to overcome such difficulties is to make use of a natural stack of the intrinsic Josephson junctions (IJJ's) in a high-T_c superconducting $Bi_2Sr_2CaCu_2O_{8+\delta}$ (BSCCO) single crystal [18], which comprises the alternating double layers of thin superconducting CuO_2 and the insulating double layers of Bi_2O_2 in a unit cell, including atomic-scale N=670 junctions in a crystal of 1 μm thick. It works as a large-scale one-dimensional natural array of identical Josephson junctions, so that it is expected to be an ideal system of intense and coherent THz sources because of the large superconducting gap energy (30~60 meV) [19]–[21]. Recently, Batov et al. and Bae et al. succeeded in the detection of sub-THz radiation, but the power was unexpect-

Manuscript received July 22, 2011.
Manuscript revised October 20, 2011.

[†]The authors are with the Institute of Materials Science, and Graduate School of Pure and Applied Sciences, University of Tsukuba, Tsukuba-shi, 305-8573 Japan, and Japan Science and Technology Agency, CREST, Kawaguchi-shi, 332-0012 Japan, and WPI-MANA.
[*]Presently, with the Quantum Beam Science Directorate, Japan Atomic Energy Agency.
a) E-mail: minami@bk.tsukuba.ac.jp

DOI: 10.1587/transele.E95.C.347

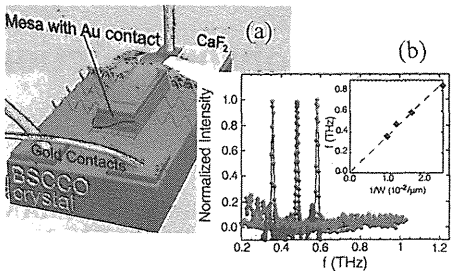

Fig. 1 (a) Schematic view of the BSCCO-based superconducting THz emitter. (b) Spectra measured by an FT-IR spectrometer. The inset shows a relation that the frequency is inversely proportional to the mesa width [24].

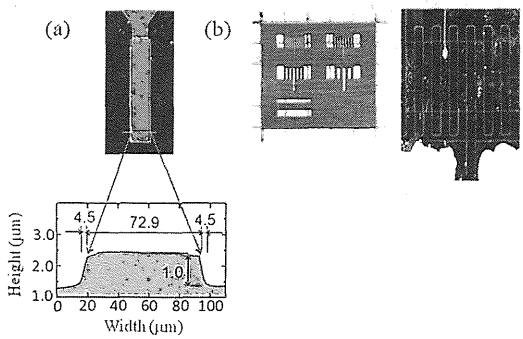

Fig. 2 (a) Photograph of a mesa fabricated by photolithography and Ar-ion milling technique, and the cross-section of the mesa observed by AFM [30]. (b) Photographs of a metal sheet of shadow masks which determine the width and length of mesas, and mesas fabricated by Ar-ion milling with the masks. The cross-sections of the mesas observed by AFM show that the edges have similar slopes as ones by photolithography.

edly small [22], [23]. Many efforts have been made in the Josephson-vortex-flow oscillator, but it was unsuccessful to make synchronization of a large number of IJJ's.

In 2007, Ozyuzer et al. have demonstrated a continuous and monochromatic THz radiation with power up to ~0.5 μW by exciting the coherent *ac*-Josephson current in the system having about 700 IJJ's in a BSCCO crystal in zero magnetic field [24]. This device was fabricated into a rectangular mesa structure on top of the single crystal of about 1 mm × 1 mm × 10 μm dimensions, as schematically shown in Fig. 1(a). The THz radiation was detected outside the cryostat after traveling in air. It was observed from early stage of experiments that the emission frequencies ranges from 0.36 to 0.85 THz, inversely proportional to the mesa width, w, which can be varied from 100 μm to 40 μm, as shown in Fig. 1(b). The emission intensity was observed to be proportional to the quadratic number of IJJ's, strongly suggesting that the emission occurs due to the coherent synchronization of the *ac*-Josephson current inside the mesa. At present, the total emission power of the BSCCO-base superconducting THz emitter have reached a few tens of μW at 0.43~0.65 THz [25], [26], and the radiation frequency ranges from 0.32 THz to 0.92 THz [27].

We review the recent experimental progress on this emitter performed at the University of Tsukuba, including the fabrication techniques, electrical and optical characteristics, synchronizing operation of two emitters, and an application to the THz imaging.

2. Fabrication Methods and Device Structures

The superconducting THz emitters are fabricated by either an Ar-ion milling or a focused ion beam (FIB) method from a piece of mm-size thin single crystal of BSCCO. High quality single crystals of BSCCO used in the present studies were prepared by a traveling solvent floating zone technique [28]. Prior to the device fabrication, the as-grown single crystals were annealed and quenched at 550~650°C in a reduced oxygen condition of 0.05~0.1% mixed with argon gas, in order to obtain slightly underdoped crystals. Terahertz emission has so far been observed with the crystals of T_c=67~89 K. The quality and the doping level of the single crystal are both crucially important for the generation of THz waves [29].

A piece of single crystal of approximately 1.0 × 1.0 mm^2 with the thickness of a few tens of μm was glued onto a sapphire substrate using a synthetic resin or silver paste. Just after cleaving the crystal using Scotch tape to obtain an atomically flat fresh surface, Ag and Au were evaporated one after another for electrodes. Then, mesa devices as shown in Fig. 2 were fabricated by an Ar-ion milling technique with photolithographic or metal masks.

Photolithography is superior to metal masks in adjusting the position of subsequent masks, but the mesa height is limited by etching of resist cover. Rectangular-shaped mesas with dimensions of the width of 40~100 μm, the length of 400 μm and the height of 1.0~2.0 μm were fabricated [24], [25], [30], [31]. It is the fabrication technique by metal masks that provides us with an easy way to obtain the reliable emitting mesas, especially when many mesas are simultaneously fabricated on a chip of BSCCO crystal to make arrayed emitters [32]. This method also enables us to make thicker mesas than the photolithographic method. Rectangular-shaped mesas with dimensions of the width of 40~120 μm, length of 200~400 μm and height of 1.0~4.0 μm were fabricated by etching step by step with the metal masks. The fabrication by the FIB technique provides us with better flexibility on the shape of mesa. Rectangular, square and disk shape mesas, etc. were fabricated by FIB technique [33]. As is easily understood, this technique is not suited for milling of wide areas, so that usually the width and the depth of the groove of about 10 μm and 1~2 μm, respectively, is cut out, finally making an island-like terrace. This technique was also used to cut out a part from rectangular mesas made by the metal-mask method so as to make them shorter or narrower [27]. By an atomic force microscope (AFM) (Keyence, VN8000/8010) observation, it turned out that the actual mesa has a trapezoidal shape with considerable slopes at their edges as seen in Fig. 2. It is interesting to note that this trapezoidal slope happens to occur in any fabrication methods so far used in our experiment. At the end of the fabrication processes, a CaF_2 film for electrical isolation and an Au film for current lead were deposited and

patterned as in Fig. 2(a), or an Au wire of 10 μm in diameter was glued by Ag paste as shown in Fig. 2(b).

3. Experiments

The THz radiation was measured by a conventional modulation technique using an optical chopper with a Si-composite bolometer filtered internally above 3 THz (IR laboratories, $f_c \approx 100$ Hz), while the current-voltage (I-V) characteristic was simultaneously measured [30]. The sample mesas were biased with a load resistor of 10~300 Ω connected in series in the current supply circuit. Because the detected signal has a large offset due to the ambient thermal radiation which is strongly absorbed by the water vapor in the atmosphere, it is important to keep dry and keep the temperature of all components constant in order to avoid a drift in the signal. The radiation spectra and the polarization were analyzed by a Fourier transformation infrared (FT-IR) spectrometer (JASCO Co., Japan, FARIS-1) incorporated with the Martin-Puplett interferometer, a modified type of the Michelson interferometer using wire-grid polarizers at the entrance, the exit and for the beam splitter, with the resolution of 7.5 GHz. A Si-composite bolometer filtered internally above 10 THz or a DLATGS pyroelectric sensor was used to detect the radiation. Spectral linewidth was estimated by using a semiconducting sub-harmonic mixer (VDI Co., USA, WR1.2SHM).

Before going into the detailed study, the temperature dependence of the mesa's c-axis resistance $R(T)$ was always measured. This gives very useful information to check the condition of the mesa such as the contact resistance, the sample quality, the doping level, and T_c, etc. This also allows us to estimate the temperature of the mesa while emitting [29], [34].

4. Optical and Electrical Characteristics: Long Rectangular Mesas

With accumulating data experimentally obtained from many IJJ mesa samples (~100), it is evident that the ac-Josephson effect, $f=(2e/h)V$, is the essential mechanism for the generation of coherent THz radiation. In order to take out the electromagnetic waves generated inside the mesa, another necessary condition is required. It is the geometrical cavity resonance necessary for the THz radiation. In almost all cases of long rectangular mesas, except for a case described later [35], the excitation of radiation has been observed in such a condition that the fundamental mode corresponding to one-half wavelength is equal to the shorter width of the mesa, w. It is expressed as $f=c_0/n\lambda=c_0/2nw$, where c_0 is the speed of light in vacuum, n the refractive index of BSCCO, and λ the wavelength of the emission in vacuum. The intense and monochromatic emission occurs, when these two conditions are simultaneously satisfied and the synchronization of all junctions in the mesa is realized. Because of the trapezoidal shape of the mesas, the central frequency of radiation changes about 10% within a variety of widths by the

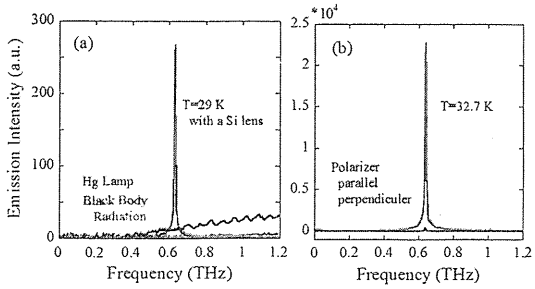

Fig. 3 Spectral characteristics of the radiation from a rectangular mesa emitter with designed dimensions of the width of 60 μm, length of 400 μm, and height of 1.9 μm. The actual mesa has a trapezoidal shape with widths of 54.6 μm at the top and 70.7 μm at the bottom. (a) The radiation is compared with those from a mercury lamp and a black body at 1200 K. A silicon hemispherical lens is inserted just in front of the sample in order to efficiently focus and collect the emitted radiation. All are measured by a DLATGS pyroelectric sensor. (b) The emission is linearly polarized with the observed polarization ratio of ~50 [31].

conditions of measurement, and is somewhat tunable by the applied voltage [36].

In Fig. 3(a), an example of the radiation from the mesa of the designed width of ~60 μm is displayed, compared with the radiations from a mercury lamp and from a black body at 1200 K [31]. A Silicon hemispherical lens is inserted just in front of the sample in order to efficiently focus and collect the emitted radiation, which increases the signal intensity by a factor of five. All radiations are analyzed by the FT-IR spectrometer and detected by a DLATGS pyroelectric sensor. The observed linewidth (full width at half maximum) of ~11 GHz is limited by the experimental resolution. Recently, the linewidth detected by the semiconducting sub-harmonic mixer has been resulted in about 0.5 GHz for a mesa emitter. The emission frequency satisfies the relation, $f=c_0/2nw$, very well, using the refractive index n ~4.2 obtained from this empirical relation which appears to work very well in many samples with different widths [37] in this sub-THz frequency region, although this value of n corresponding to the dielectric constant $\epsilon=17.6$ is about 50% larger than that ($\epsilon=12$) obtained previously by infrared spectroscopy [38].

The intensity is much higher than that of the mercury lamp which is widely used for a far infrared light source, so that the radiation is detectable by such a sensor which works at room temperature without using any sophisticated detection system. The total radiation power emitted was estimated to be ~5 μW [30], [31]. For typical values of radiation power, 1~10 μW is commonly obtained at the frequencies up to 0.65 THz, which is also checked by an InSb hot-electron detector whose system sensitivity is provided by the supplier (QMC). Since the total power fed into mesas is approximately 3~30 mW, this results in the total efficiency of radiation to be ~10^{-3}.

Observed resonance condition for the rectangular mesas appears to be rather peculiar, because it is in general easily found that the excitation energy of the cavity resonance for the longer dimension is lower than that for the shorter one, although the Josephson plasma frequency,

$f=c_0/2\pi n\lambda_c$ where λ_c is the c-axis superconducting penetration depth, may be the lower cutoff frequency. Actually, the radiation according to different resonance conditions from above has been recently observed. Wang et al. have reported the THz radiation at high bias current whose radiation frequency varies in a wide range strongly depending on temperature, suggesting a different resonance mechanism for locking into a certain frequency associated with local and modulated self-heating phenomena [35]. Another exceptional case is seen when the external structure out of a mesa works as a resonator [27]. Further, the radiation tunable in wide frequency range has been observed in the inner branch states, whose resonance condition for locking into a certain frequency is not yet understood well [39]. In short rectangular, square and disk mesas, various resonant cavity modes determined by the geometry have been observed so far [33].

Figure 3(b) shows the experimentally observed spectra measured at perpendicular and parallel settings of a pair of the wire-grid polarizers at the entrance and exit of the Martin-Puplett interferometer with respect to the *ab*-plane of the BSCCO crystal. The THz radiation emitted from the mesa emitter is linearly polarized with the polarization direction of the electric field being perpendicular to the *ab*-plane of the BSCCO crystal.

When all junctions are active, the emission voltage is given by $V_{em}=(c_0h/2e)(1/nl_c)(d/w)$, where l_c=30.7 Å is the c-axis length of BSCCO and d the height of the mesa. This can simply be expressed as $V_{em}=48.2(d/w)$ (V) after numerical manipulation. This means that the voltage required for the emission depends only on the dimensions of the mesa; the height d and the width w. When only a part of the IJJ's is active, d should be replaced by the effective thickness. On the other hand, the I-V characteristic of the mesa strongly depends on the doping level of the crystal and the temperature of the mesa, in addition to the dimensions. For most of the mesa emitters, the local heating of the mesa due to self-heating produces the negative differential resistance (NDR) in the high electric current region. Therefore, there are two regions in the I-V curve where strong THz radiation can be generated: one is located in the return branch in the hysteretic I-V curve as seen in Fig. 4(a) [24] and another appears in the region of NDR at high electric currents as seen in Fig. 4(b) [29]. The former has more often been observed for underdoped crystals of T_c=67~85 K, whereas the latter has been observed for more lightly underdoped crystals of T_c=80~89 K [29]. It is just because the I-V curve crosses V_{em} at high electric currents only for lightly underdoped crystals as seen in Fig. 4. For lightly underdoped crystals, the emission often appears in both regions in the I-V curve.

The emission appearing in the return branches occurs in many cases in the vicinity of a jump to the other stable branches, and stops radiating when the I-V curve is exerted to the jump, as seen around 0.71 V in Fig. 4(a). This process is irreversible, and in order to get the emission again, it is necessary to go around the outermost branch and come back to the same bias point. We call this type of emission the irreversible (IR-) type of radiation. As the highest emission

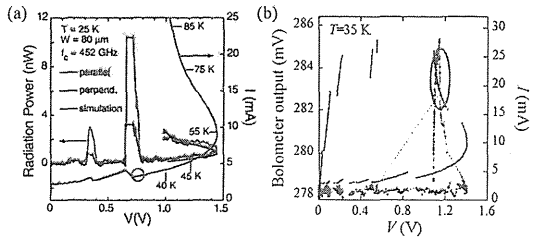

Fig. 4 (a) The I-V characteristic and radiation power of an IR-type 80 μm mesa emitter. The radiation frequency is 0.48 THz. The voltage dependences of the current and of the radiation power for parallel and perpendicular settings of the filter with 0.452 THz cut-off frequency are shown for decreasing bias. Polarized emission occurs near 0.71 and 0.37 V, and unpolarized thermal radiation occurs at higher bias [24]. (b) The I-V and radiation characteristics of an R-type 60 μm mesa [29]. The emission spectra measured by the FT-IR spectrometer show a sharp peak of the fundamental radiation at 0.64 THz which satisfies the relation $f=c_0/2nw$. The bolometer signal has a big offset due to the ambient thermal radiation modulated by an optical chopper.

usually occurs in the vicinity of the unexpected jump, it is rather difficult to stabilize the emission.

Figure 4(b) shows the I-V curve and the radiation characteristic of a 60 μm mesa emitter (actual dimensions measured by AFM are 53 μm at the top and 61 μm at the bottom of the width, 350 μm in length and 1.3 μm in height.) [29]. The emission in this particular mesa occurs in the region of NDR at high currents. The emission at 0.64 THz obeys two necessary conditions similar to the IR-type emission: the *ac*-Josephson effect and the cavity resonance for the narrower width, $f=c_0/2nw$. Wang et al. also has confirmed the emission at high bias currents, however, they suggested a different resonance mechanism from the mentioned above [35]. The emitting voltage V_{em} ~1.15 V implies that almost all junctions are active and participate in the synchronized emission. The resistance of the mesa at the maximum intensity of radiation can be estimated to be 57 Ω from the I-V curve. Comparing it with the $R(T)$ curve, it turns out that the emission occurs when the mesa temperature is just below T_c. In this region, both electric current and radiation power are continuous and reversible functions of voltage around the maximum intensity of radiation. We therefore call this type of emission as the reversible (R-) type of radiation. The discontinuity around V=1.25~1.35 V is because the slope of the I-V curve is smaller than that of the load line. From device application point of view, the R-type is superior to the IR-type in stability, reproducibility, simplicity of bias operation and easy to use in power modulation technique, but the power consumption is much larger.

Figures 5(a) and 5(b) present the angle θ dependences of the radiation intensity, $I(\theta)$, in the yz-plane and the xz-plane, respectively, for a long rectangular mesa with the length~400 μm and width~60 μm [37]. Here, the xyz-coordinate system is defined as in Fig. 5(c): the x-axis is parallel to the long side of the mesa and the z-axis is perpendicular to the surface, and θ is the angle from the z-axis. The observed radiation is very anisotropic: it is the strongest in the yz-plane and mostly several times weaker in xz-plane for long rectangular mesas. The maximum intensity I_{max} oc-

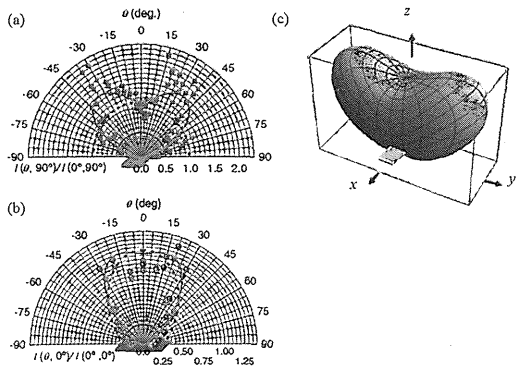

Fig. 5 Polar plots of the radiation intensities $I(\theta)$ normalized at $I(0)$ measured in the yz-plane (a) and the xz-plane (b) for a long rectangular mesa emitter. The xyz-coordinate system is defined as sketched in (c) and θ is the angle from the z-axis. The 3D plot of the spatial distribution of radiation predicted by a dual-source mechanism is sketched in (c) with adjusting the relative amplitude and phase of the two source currents and accounting for the substrate effect. The solid curves in (a) and (b) are cross-sectional cuts of the 3D plot by the yz-plane and the xz-plane, respectively. The dashed curves are the corresponding cavity model fits (see text) [37].

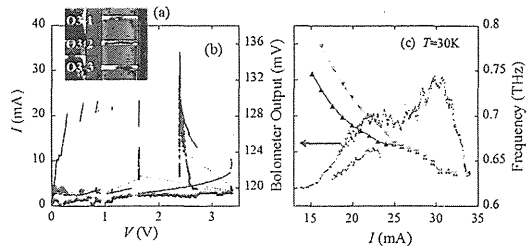

Fig. 6 (a) A photograph of the sample in which three mesas were fabricated on the surface of a BSCCO single crystal. A gold wire of 10 μm in diameter was attached to each mesa by silver paste [32]. (b) The I-V curve and radiation power characteristic as a function of voltage when the O3-2 and O3-3 mesas are biased in series. (c) The radiation frequency and radiation power as a function of current when the O3-2 and O3-3 mesas are biased in series. The bolometer signal includes little increased offset at higher bias current due to the thermal radiation from the sample.

curs at $\theta \sim \pm 30°$ from the mesa top (θ=0°) in the yz-plane. At the top of the mesa, the radiation intensity has a local minimum with $I(0)/I_{max} \approx 0.4 \sim 0.7$. On the other hand, the observed $I(\theta)$ diminishes strongly as $\theta \rightarrow 90°$ (parallel to the xy-plane; the ab-plane of BSCCO crystal). Although there is some sample-to-sample variation, the similar behaviors are obtained for long rectangular mesa emitters [31].

If the radiation were simply induced by the fundamental cavity resonance mode, as expected from capacitor patch antenna theory [40] and widely predicted for rectangular BSCCO mesas [41]–[46], $I(\theta)$ would be maximal at θ=0° as shown by the dashed curves in Figs. 5(a) and 5(b). If a uniform ac-Josephson current were the primary radiation source, $I(\theta)$ would vanish at θ=0° and be maximal near to θ=90°, as for simple dipole radiation [40]. Apparently, the experimental results contradict both simple explanations. In order to explain the experimental results, a dual-source mechanism has been proposed by Klemm and Kadowaki [47], [48], in which the uniform and inhomogeneous parts of the ac-Josephson current respectively act as an electric surface current source and set up a displacement current that excites a mesa cavity resonance mode which locks the radiation frequency, and acts as a magnetic surface current source. By adjusting the relative amplitude and phase of the two source currents and accounting for the substrate effect, excellent agreement with experimental results is obtained as depicted by the solid curves in Figs. 5(a) and 5(b) and sketched in Fig. 5(c) [37].

5. Synchronization of Two Emitters Fabricated on a BSCCO Crystal

The BSCCO-base mesa emitter can be viewed as a large scale array of strongly coupled Josephson junctions stacked in the direction of the height. It is expected that the radiation power is proportional to N^2, if the N junctions work coherently [6], [7], [14], [17], [24]. However, there would be a limitation in mesa height, because this device is highly dissipative with poor thermal conductivity of BSCCO so that the mesa gets heated easily above T_c. A solution to overcome this problem and to enhance the radiation power greatly may be to construct 1D or 2D planer array of mesas like the arrays of Nb-base discrete Josephson junctions. Similar to the previous observation [8], Orita et al. demonstrated synchronized operation between two rectangular emitting mesas separately located side by side at a distance of 200 μm on a BSCCO single crystal [32].

Figure 6(a) shows a photograph of the sample mesas which were made on the surface of a BSCCO crystal and located side by side at a distance of 200 μm. By the AFM measurement, the widths were 47, 53 and 52 μm at the top and 55, 61 and 60 μm at the bottom for O3-1, O3-2 and O3-3 mesas, respectively. The length was 400 μm and the height was 1.3 μm for three mesas. When the mesas are individually biased, the radiation frequencies are 0.73, 0.63 and 0.68 THz for O3-1, O3-2 and O3-3 mesas, respectively.

Figure 6(b) shows the I-V curve and the radiation intensity as a function of voltage when the O3-2 and O3-3 mesas are biased in series. The I-V curve exhibits a characteristic hysteresis of the IJJ system, and a negative differential resistance due to Joule heating in the high bias current region. Around $V \approx 1.6$ V, only the O3-3 mesa emits because the superconducting critical current is lower than O3-2. Then, both mesas start to emit radiation around $V \approx 2.4$ V. The R-type radiation occurs in the high current region of the outermost reversible branch at the frequency around 0.7 THz.

Figure 6(c) shows the radiation frequency and radiation power as a function of current at 30 K when the O3-2 and O3-3 mesas are biased in series. The radiation occurs in the wide range of bias current of 15~33 mA. The spectra have two peaks in the bias current below 25 mA, while they merge into one line in the range of bias current above 26 mA and stay together until the emission stops by Joule heating. The radiation intensity integrated for two separated lines increases with increasing current and takes a constant

intensity between 22 and 26 mA. With further increase of the current, the radiation intensity increases again to a maximum value of 1.5 times of the constant intensity between 22 and 26 mA. This means that two separated mesas coherently work as a strongly connected THz emitter, probably by the synchronized terahertz current propagating through the superconducting substrate. The power observed here is not quite $4(=2^2)$ times as expected, but it was about 3 times.

6. Electrical Modulation of the Radiation Intensity and the Application to THz Imaging

The R-type emitter allows us to operate it as a power modulation mode by simply applying a voltage to switch bias point from one to the other. Electrical modulation is a very efficient technique to reduce noise and it is crucially important for applications of this device. Here, we present the demonstration of the modulated radiation intensity at low-frequency and the application to the raster-scan imaging.

For the amplitude modulation (or switching) of the radiation, the bias current was directly modulated with a rectangular pulse together with an appropriate *dc* current. The THz radiation was detected by an InSb hot-electron detector (QMC, f_c ≈500 kHz). Figure 7(a) shows the THz output signal (bottom) from a mesa emitter (width: 60 μm, length: 350 μm, height: 1.3 μm) on the oscilloscope screen. The radiation frequency is 0.58 THz. The bias current is modulated with a small-amplitude (top) of 1.8 mA around the emitting condition around I=16~30 mA. The modulation frequency is 20 kHz. For small current modulation, the modulation up to 500 kHz is observed.

Using the amplitude modulation of radiation, we demonstrate that it is possible to use the BSCCO-base THz emitter for an application to the raster-scan imaging. The optical set-up is displayed in Fig. 7(b). The THz radiation emitted from a cooled emitter comes out from the cryostat through a quartz-glass window and is focused at a sample mounted on a controllable stage by two off-axial parabolic mirrors. The transmitted THz beam is detected by the InSb hot-electron detector placed behind the sample. The positions of optical elements were adjusted by using a visible light beam of a LED mounted on the other side of the cold finger on which the THz emitter is mounted.

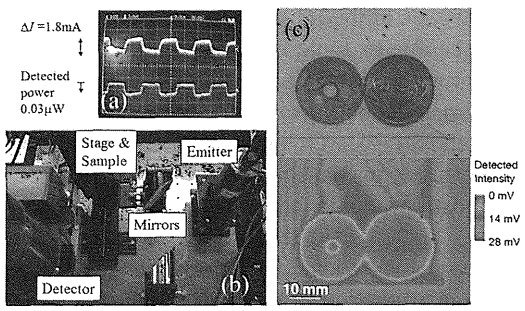

Fig. 7 (a) An oscillograph of the THz output signal from a 60 μm mesa emitter detected by an InSb hot-electron detector (bottom) for a small-amplitude current modulation (top) around the emitting condition. The modulation frequency is 20 kHz. (b) Optical set-up used for the raster-scan imaging. (c) A transmitted THz image of two Japanese coins put in a brownish envelope, with the photograph by visible light where the coins are put out of the envelope. Interference pattern produced by paper sheets of the envelope is clearly visible.

Since the InSb hot-electron detector has the lowest noise of 3 nV/Hz$^{1/2}$ around 20 kHz (30 nV/Hz$^{1/2}$ at 100 Hz, ≥100 nV/Hz$^{1/2}$ at *dc*), the R-type THz emitter is modulated at 20 kHz. The modulation frequency also matches our targets of the scan speed and spatial resolution. The signal is pre-amplified with the gain of 1000 and is detected by a lock-in amplifier with the time constant of 1~5 ms, so that the noise voltage of V_{rms} ≈0.1 mV is estimated. All the control of the movable stage and the measuring instruments and the acquisition and processing of the data are automatically performed by a personal computer.

A transmitted THz image of two Japanese coins put in a brownish envelope is displayed in Fig. 7(c), with the photograph by visible light where the coins are put out of the envelope. The frequency of THz radiation is 0.56 THz. The interference pattern produced by two paper sheets of the brownish envelope and the coins with thickness of 1.5 mm is clearly visible, demonstrating that the radiation is stable and monochromatic. A coin has a hole of 5 mm exactly. We estimate the spatial resolution at ~1.3 mm. Signal voltage of 28 mV$_{rms}$ without sample is obtained at the input of the lock-in amplifier, corresponding to 24 nW of detected radiation power. The total power emitted is estimated at ~1 μW, taking into account the solid angle to the first mirror and the transmittance of the quartz-glass window of cryostat. Short-time noise voltage was ~0.2 mV$_{rms}$, corresponding to the detector noise. It takes 45 minutes to get this image at present, however, it may be possible to improve much with the same S/N ratio and the spatial resolution in the near future.

7. Summary and Future Perspectives

The intrinsic Josephson junction system in a high-T_c superconductor $Bi_2Sr_2CaCu_2O_{8+\delta}$ works as an array of strongly coupled Josephson junctions made of a high-T_c superconductor, which gives us a solution to resolve the difficulty in fabrication of an artificial array from discrete high-T_c Josephson junctions due to the extremely short coherence length. As a result, a remarkable phenomenon, monochromatic and continuous radiation with high power at sub-THz frequency region, has been achieved by fabricating it into mesa structure. This emission has been understood by the coherently synchronized oscillation of Josephson current excited across large numbers of the intrinsic Josephson junctions. By tuning at a variety of cavity resonance modes, the emission has been observed at the frequency range of 0.32~0.92 THz, and the total emission power has reached a few tens of μW at 0.43~0.65 THz with the frequency purity of 0.5 GHz. There are two regions in the I-V curve where strong THz radiation can be generated: one is located in the return branch in the hysteretic I-V curve (IR-type), while another radiation occurs in the negative differential resistance

region at high bias currents (R-type).

The application to the raster-scan imaging has directly demonstrated the intensity, monochromatic nature and stability of the radiation under electrical switching operation. However, the radiation power is still insufficient for real-time imaging, and the frequency purity is too low to use it for local oscillator of receiver. We believe that the development of planer array formation of mesas and the improvement in the performance of individual mesa device are necessary. As a beginning, we have demonstrated the synchronization of two emitters located on a chip of crystal. Aiming at practical uses, the research of high-speed modulation and electrical tuning of radiation frequency may also be important. This all-high-T_c superconductor device, with a miniature size of ~1 mm dimensions, has the advantage of operating at higher temperature more than 30 K. This may allow us to use the compact Stirling coolers and make a portable THz-light source and a compact imaging system, etc. We expect that this THz emitter can widely be used in research fields and also for practical purposes.

Acknowledgments

The authors would like to express our special thanks to Profs. M. Tachiki, R.A. Klemm, I. Kakeya, L. Ozyuzer, U. Welp, W.-K. Kwok, Drs. K. Yamaki, H. Asai, Mrs. H. Yamaguchi, K. Delfanazari, T. Koike, N. Orita, and M. Sawamura for close collaborations.

References

[1] M. Tonouchi, "Cutting-edge terahertz technology," Nature Photonics, vol.1, pp.97–105, 2007.

[2] D.L. Woolard, W.R. Loerop, and M.S. Shur, eds., Terahertz sensing Technology, World Scientific, Singapore, 2002.

[3] D.N. Langenberg, D.J. Scalapino, B.N. Taylor, and R.E. Eck, "Investigation of microwave radiation emitted by Josephson junctions," Phys. Rev. Lett., vol.15, pp.294–297, 1965.

[4] A.H. Dayem and C.C. Grimes, "Microwave emission from superconducting point-contacts," Appl. Phys. Lett., vol.9, pp.47–49, 1966.

[5] J.E. Zimmerman, J.A. Cowen, and A.H. Silver, "Coherent radiation from voltage-biased weakly connected superconductors," Appl. Phys. Lett., vol.9, pp.353–355, 1966.

[6] T.F. Finnegan and S. Waflsten, "Observation of coherent microwave radiation emitted by coupled Josephson junctions," Appl. Phys. Lett., vol.21, pp.541–544, 1972.

[7] C. Varmazis, R.D. Sandell, A.K. Jain, and J.E. Lukens, "Generation of coherent tunable Josephson radiation at microwave frequencies with narrowed linewidth," Appl. Phys. Lett., vol.33, pp.357–359, 1978.

[8] R.D. Sandell, C. Varmazis, A.K. Jain, and J.E. Lukens, "Study of the properties of coherent microbridges coupled by external shunts," AIP Conf. Proc. no.44, Future Trends in Superconductive Electronics (AIP, 1978), pp.327–334.

[9] A.K. Jain, K.K. Likharev, J.E. Lukens, and J.E. Sauvageau, "Mutual phase-locking in Josephson junction arrays," Phys. Rep., vol.109, pp.309–426, 1984.

[10] S. Han, B. Bi, W. Zhang, and J.E. Lukens, "Demonstration of Josephson effect submillimeter wave sources with increased power," Appl. Phys. Lett., vol.64, pp.1424–1426, 1994.

[11] P.A.A. Booi and S.P. Benz, "High power generation with distributed Josephson-junction arrays," Appl. Phys. Lett., vol.68, pp.3799–3801, 1996.

[12] S. Kiryu, W. Zhang, S. Han, S. Deus, and J.E. Lukens, "Off-chip detection of radiation from a linear array oscillator with a spiral antenna," IEEE Trans. Appl. Supercond., vol.7, pp.3107–3110, 1997.

[13] M. Darula, T. Doderer, and S. Beuven, "Millimetre and sub-mm wavelength radiation sources based on discrete Josephson junction arrays," Supercond. Sci. Technol., vol.12, pp.R1–R25, 1999.

[14] P. Barbara, A.B. Cawthorne, S.V. Shitov, and C.J. Lobb, "Stimulated emission and amplification in Josephson junction arrays," Phys. Rev. Lett., vol.82, pp.1963–1966, 1999.

[15] V.P. Koshelets and S.V. Shitov, "Integrated superconducting receivers," Supercond. Sci. Technol., vol.13, pp.R53–R69, 2000.

[16] B. Vasilić, S.V. Shitov, C.J. Lobb, and P. Barbara, "Josephson-junction arrays as high-efficiency sources of coherent millimeter-wave radiation," Appl. Phys. Lett., vol.78, pp.1137–1139, 2001.

[17] F. Song, F. Müller, R. Behr, and A.M. Klushin, "Coherent emission from large arrays of discrete Josephson junctions," Appl. Phys. Lett., vol.95, 172501, 2009.

[18] R. Kleiner, F. Steinmeyer, G. Kunkel, and P. Müller, "Intrinsic Josephson effects in $Bi_2Sr_2CaCu_2O_8$ single crystals," Phys. Rev. Lett., vol.68, pp.2394–2397, 1992.

[19] T. Koyama and M. Tachiki, "Plasma excitation by vortex flow," Solid State Commun., vol.96, pp.367–371, 1995.

[20] M. Tachiki, M. Iizuka, K. Minami, S. Tejima, and H. Nakamura, "Emission of continuous coherent terahertz waves with tunable frequency by intrinsic Josephson junctions," Phys. Rev. B, vol.71, 134515, 2005.

[21] S. Savel'ev, A.L. Rakhmanov, and F. Nori, "Using Josephson vortex lattices to control terahertz radiation: Tunable transparency and terahertz photonic crystals," Phys. Rev. Lett., vol.94, 157004, 2005.

[22] I.E. Batov, X.Y. Jin, S.V. Shitov, Y. Koval, P. Müller, and A.V. Ustinov, "Detection of 0.5 THz radiation from intrinsic $Bi_2Sr_2CaCu_2O_8$ Josephson junctions," Appl. Phys. Lett., vol.88, 262504, 2006.

[23] M.H. Bae, H.J. Lee, and J.H. Choi, "Josephson-vortex-flow terahertz emission in layered high-Tc superconducting single crystals," Phys. Rev. Lett., vol.98, 027002, 2007.

[24] L. Ozyuzer, A.E. Koshelev, C. Kurter, N. Gopalsami, Q. Li, M. Tachiki, K. Kadowaki, T. Yamamoto, H. Minami, H. Yamaguchi, T. Tachiki, K.E. Gray, W.-K. Kwok, and U. Welp, "Emission of coherent THz radiation from superconductors," Science, vol.318, pp.1291–1293, 2007.

[25] K. Yamaki, M. Tsujimoto, T. Yamamoto, A. Furukawa, T. Kashiwagi, H. Minami, and K. Kadowaki, "High-power terahertz electromagnetic wave emission from high-T_c superconducting $Bi_2Sr_2CaCu_2O_{8+\delta}$ mesa structures," Opt. Express, vol.19, pp.3193–3201, 2011.

[26] T. Yamamoto, private communication.

[27] T. Kashiwagi, K. Yamaki, M. Tsujimoto, K. Deguchi, N. Orita, T. Koike, R. Nakayama, H. Minami, T. Yamamoto, R.A. Klemm, M. Tachiki, and K. Kadowaki, "Geometrical full-wavelength resonance mode generating terahertz waves from a single crystalline $Bi_2Sr_2CaCu_2O_{8+\delta}$ rectangular mesa," J. Phys. Soc. Jpn., vol.80, 094709, 2011.

[28] T. Mochiku and K. Kadowaki, "Growth and properties of $Bi_2Sr_2(Ca,Y)Cu_2O_{8+\delta}$ single crystals," Physica C, vol.235-240, pp.523–524, 1994.

[29] H. Minami, N. Orita, T. Koike, T. Yamamoto, and K. Kadowaki, "Continuous and reversible operation of Bi2212 based THz emitters just below T_c," Physica C, vol.470, pp.S822–S823, 2010.

[30] K. Kadowaki, H. Yamaguchi, K. Kawamata, T. Yamamoto, H. Minami, I. Kakeya, U. Welp, L. Ozyuzer, A.E. Koshelev, C. Kurter, K.E. Gray, and W.-K. Kwok, "Direct observation of terahertz electromagnetic waves emitted from intrinsic Josephson junctions in single crystalline $Bi_2Sr_2CaCu_2O_{8+\delta}$," Physica C, vol.468, pp.634–639, 2008.

[31] H. Minami, I. Kakeya, H. Yamaguchi, T. Yamamoto, and K. Kadowaki, "Characteristics of terahertz radiation emitted from the intrinsic Josephson junctions in high-T_c superconductor $Bi_2Sr_2CaCu_2O_{8+\delta}$," Appl. Phys. Lett., vol.95, 232511, 2009.
[32] N. Orita, H. Minami, T. Koike, T. Yamamoto, and K. Kadowaki, "Synchronized operation of two serially connected Bi2212 THz emitters," Physica C, vol.470, pp.S786–S787, 2010.
[33] M. Tsujimoto, K. Yamaki, K. Deguchi, T. Yamamoto, T. Kashiwagi, H. Minami, M. Tachiki, K. Kadowaki, and R.A. Klemm, "Geometrical resonance conditions for THz radiation from the intrinsic Josephson junctions in $Bi_2Sr_2CaCu_2O_{8+\delta}$," Phys. Rev. Lett., vol.105, 037005, 2010.
[34] C. Kurter, K.E. Gray, J.F. Zasadzinski, L. Ozyuzer, A.E. Koshelev, Q. Li, T. Yamamoto, K. Kadowaki, W.-K. Kwok, M. Tachiki, and U. Welp, "Thermal management in large Bi2212 mesas used for terahertz sources," IEEE Trans. Appl. Supercond., vol.19, pp.428–431, 2009.
[35] H.B. Wang, S. Guenon, B. Gross, J. Yuan, Z.G. Jiang, Y.Y. Zhong, M. Grunzweig, A. Iishi, P.H. Wu, T. Hatano, D. Koelle, and R. Kleiner, "Coherent terahertz emission of intrinsic Josephson junction stacks in the hot spot regime," Phys. Rev. Lett., vol.105, 057002, 2010.
[36] K.E. Gray, A.E. Koshelev, C. Kurter, K. Kadowaki, T. Yamamoto, H. Minami, H. Yamaguchi, M. Tachiki, W.-K. Kwok, and U. Welp, "Emission of terahertz waves from stacks of intrinsic Josephson junctions," IEEE Trans. Appl. Supercond., vol.19, pp.886–890, 2009.
[37] K. Kadowaki, M. Tsujimoto, K. Yamaki, T. Yamamoto, T. Kashiwagi, H. Minami, M. Tachiki, and R.A. Klemm, "Evidence for dual-source mechanism of THz radiation from rectangular mesa of single crystalline $Bi_2Sr_2CaCu_2O_{8+\delta}$ intrinsic Josephson junctions," J. Phys. Soc. Jpn., vol.79, 023703, 2010.
[38] S. Tajima, G.D. Gu, S. Miyamoto, A. Odagawa, and N. Koshizuka, "Optical evidence for strong anisotropy in the normal and superconducting states in $Bi_2Sr_2CaCu_2O_{8+z}$," Phys. Rev. B, vol.48, pp.16164–16167, 1993.
[39] M. Tsujimoto, T. Yamamoto, K. Delfanazari, R. Nakayama, T. Kitamura, M. Sawamura, T. Kashiwagi, H. Minami, M. Tachiki, K. Kadowaki, and R.A. Klemm, "Broadly tunable sub-terahertz emission from internal branches of the current-voltage characteristics of superconducting Bi2Sr2CaCu08+δ single crystals," to be published in Phys. Rev. Lett., 2012.
[40] C.A. Balanis, Antenna Theory, Analysis and Design, 3rd ed., Wiley, Hoboken, NJ, 2005.
[41] L.N. Bulaevskii and A.E. Koshelev, "Radiation due to Josephson oscillations in layered superconductors," Phys. Rev. Lett., vol.99, 057002, 2007.
[42] A.E. Koshelev and L.N. Bulaevskii, "Resonant electromagnetic emission from intrinsic Josephson-junction stacks with laterally modulated Josephson critical current," Phys. Rev. B, vol.77, 014530, 2008.
[43] S. Lin, X. Hu, and M. Tachiki, "Computer simulation on terahertz emission from intrinsic Josephson junctions of high-T_c superconductors," Phys. Rev. B, vol.77, 014507, 2008.
[44] S. Lin and X. Hu, "Possible dynamic state in inductively coupled intrinsic Josephson junctions of layered high-T_c superconductors," Phys. Rev. Lett., vol.100, 247006, 2008.
[45] X. Hu and S. Lin, "Three-dimensional phase-kink state in a thick stack of Josephson junctions and terahertz radiation," Phys. Rev. B, vol.78, 134510, 2008.
[46] A.E. Koshelev, "Alternating dynamic state self-generated by internal resonance in stacks of intrinsic Josephson junctions," Phys. Rev. B, vol.78, 174509, 2008.
[47] R.A. Klemm and K. Kadowaki, "Angular dependence of the radiation power of a Josephson STAR-emitter," J. Supercond. Nov. Magn., vol.23, pp.613–616, 2010.
[48] R.A. Klemm and K. Kadowaki, "Output from a Josephson stimulated terahertz amplified radiation emitter," J. Phys.: Condens. Matter, vol.22, 375701, 2010.

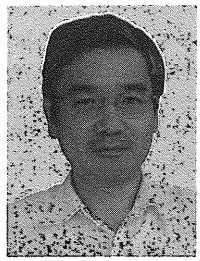

Hidetoshi Minami received the Ph.D. degree in Physics from University of Tokyo in 1992. After Assistant Professor of Department of Pure and Applied Sciences, University of Tokyo (1986–1992), then Lecturer of Institute of Materials Science, University of Tsukuba (1992–).

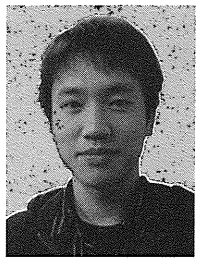

Manabu Tsujimoto received the Master's degree in Engineering from University of Tsukuba in 2010, then entered Graduate School of Pure and Applied Sciences, Doctoral Program in Material Science, University of Tsukuba in 2010. During 2010–2011, he was Research Assistant in University of Tsukuba. He is now Research Fellow of the Japan Society for the Promotion of Science (2011–).

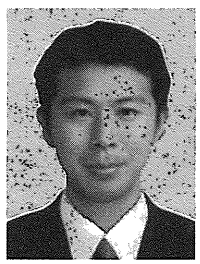

Takanari Kashiwagi received the Ph.D. degree in Physics from Osaka University in 2008. After Post. Doc. in Center for Quantum Science and Technology under Extreme Conditions in Osaka University (2008–2009), then Assistant Professor of Institute of Materials Science, University of Tsukuba (2009–).

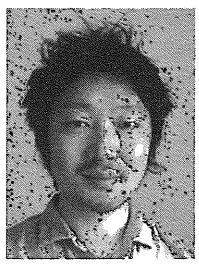

Takashi Yamamoto received the Ph.D. degree in Engineering from University of Tsukuba in 2007. Postdoctoral Fellow in Institute of Materials Science, University of Tsukuba (2007–2011). Currently, Postdoctoral Fellow in Quantum Beam Science Directorate, Japan Atomic Energy Agency (2011–).

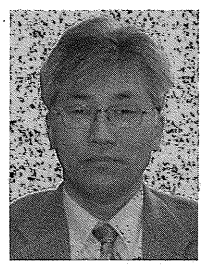

Kazuo Kadowaki received the Ph.D. degree in Physics from Osaka University in 1980. After Post. Doc. in Department of Physics, Alberta University, Canada (1982–1986), and lecturer in Natuurkundig Laboratorium der Universiteit van Amsterdam, the Netherlands (1986–1990), group leader in National Research Institute for Metals (1990–1995), Assistant Professor, then Professor of Institute of Materials Science, University of Tsukuba (1995–).